LABORATORY SPACE WEATHERING INDUCED FORMATION OF SULFIDES IN THE MURCHISON (CM2) METEORITE. J. J. Gillis-Davis[1], C. Zhu[2], S. Góbi[3], M. J. Abplanalp[2], R. Frigge[2], and R. I. Kaiser[2]. [1]Hawaii Institute of Geophysics and Planetology, Department of Chemistry, 1680 East-West Road University of Hawaii at Mānoa, Honolulu, HI 96822, USA (gillis@higp.hawaii.edu), [2]Department of Chemistry, University of Hawaii at Mānoa, Honolulu, HI 96822, USA, [3]Department of Chemistry, University of Coimbra, 3004–535, Coimbra, Portugal.

Introduction: Space weathering alters the physical, spectral, and chemical properties of surfaces of atmosphere-free bodies. The main components of space weathering are radiation (e.g., solar wind, cosmic ray, and photon) and meteoroid/micrometeorite bombardment. The Moon is the archetype example for resolving many mysteries of the space-weathering effects (e.g., exposure to space causes the regolith to darken, redden, and lose spectral contrast [1,2]). Space weathering also occurs on S-complex asteroids [3], and it is often presumed that a lunar-style of space weathering is relevant to asteroids. However, differences in spectral trends and albedo variations between S-complex asteroids (e.g., 243 Ida, 433 Eros, 951 Gaspra, and 25143 Itokawa) suggests that target composition and/or space weathering style plays an important in space weathering effects (e.g., [4-6]). Therefore, the Moon, which is relatively depleted vapor-mobilized elements such as sulfur [7], has limited applicability to understanding space weathering effects of sulfur compounds on primitive/undifferentiated asteroids. While some experimental and theoretical work has been done with respect to studying sulfur mobilization on S-complex asteroids [8-10], understanding space weathering effects related to sulfur containing species for C-complex asteroids is only in the beginning stages. Studies of sulfur mobilization are needed for interpreting measurements of C-complex asteroids <500 km: e.g., OSIRIS-Rex at 101955 Bennu (B-type), and Hayabusa-2 analyses of 162173 Ryugu (C-type).

X-ray (XRS) and neutron spectrometer analyses of planetary surfaces can measure elemental compositions for comparison with meteorites [11,12]. As compositional data for Bennu and Ryugu is forthcoming, we use sulfur compositions measured for two S-type asteroids: Eros and Itokawa. The Near Earth Asteroid Rendezvous (NEAR) XRS data revealed that ratios among Al, Mg, Fe, and Si are similar to those found in L and LL chondrite meteorites [13], however, XRS-derived S/Si values are an order of magnitude lower than typical values for L and LL Ordinary Chondrites (OC) [13-16]. Similarly, XRS data from the Hayabusa-1 spacecraft measured a lower or equal sulfur abundance relative to the average abundance in OC depending on sampling point for Itokawa [15]. Further, energy-dispersive X-ray surface mapping of particle RA-QD02-0125, returned by the Hayabusa mission, shows sulfur depletion as well [18].

Hence, experimental [8,9], theoretical modelling [10], remote sensing [13-17], and sample [18,19] evidence supports that the S depletion is due to space weathering. This work extends the current state of knowledge by reporting results from the exposure of Murchison meteorite powder to energetic electrons and laser heating to elucidate the mobilization of sulfur from its non-volatile forms (e.g., troilite FeS, pyrrhotite $Fe_{1-x}S$, pentlandite $(Fe,Ni)_9S_8$, and murchisite Cr_5S_6).

Methods: Experiments were conducted in a contamination-free ultrahigh vacuum (UHV) stainless chamber evacuated to a base pressure of a few 10^{-11} Torr. Murchison meteorite powder with a grain size of <45 µm was pressed onto a silver mirror substrate (thickness 57±7 µm or 0.0306 g). A cold finger, which is interfaced with the mirror, is cooled by a closed-cycle helium compressor. Temperature is maintained between 5.5±0.1 K and 300.0 by a cartridge heater connected to a programmable temperature controller.

Samples were cooled to either 5.5 or 150 K whereupon it was simultaneously irradiated by infrared pulsed CO_2 laser (10.6 µm@ 10 W cm^{-2} for 5 hours) and by energetic electrons with an energy of 5 keV @ 10 µA for 5 hours. Infrared laser and energetic electron irradiations simulate thermal effects of micrometeorite bombardments and secondary electrons released during galactic cosmic rays and high energy solar wind particles on airless bodies, respectively. The irradiated samples were kept at 5.5 or 150.0 K for one hour post irradiation and then warmed up to 300 K at a rate of 1 K min^{-1} (temperature programmed desorption; TPD). The TPD profiles of the sublimed molecules from the irradiated samples from both temperatures were collected via photoionization reflectron time-of-flight mass spectrometry (PI-ReTOF-MS). This technique uses pulsed coherent vacuum ultraviolet light at 118.2 nm (10.49 eV) to ionize the subliming molecules. The ionized molecules were mass analyzed with a ReTOF mass spectrometer based on the arrival time to a multichannel plate.

Results & Discussion: Figure 1 depicts the intensities of the mass-to-charge ratios up to m/z = 100 as a function of the temperature during the TPD phase of the unirradiated (blank) and dual irradiated (5.5 and 150 K) Murchison samples recorded via PI-ReTOF-MS. No signal was detected in the blank experiment (Figure 1(a)), which confirms that the peaks observed in the irradiation experiments originate from irradiation of the samples and not from a TPD heating to 300 K. The PI-ReTOF-MS data exhibit more complexity and greater yields at a higher irradiation temperature. The high temperature irradiations generated appreciably more H_2S

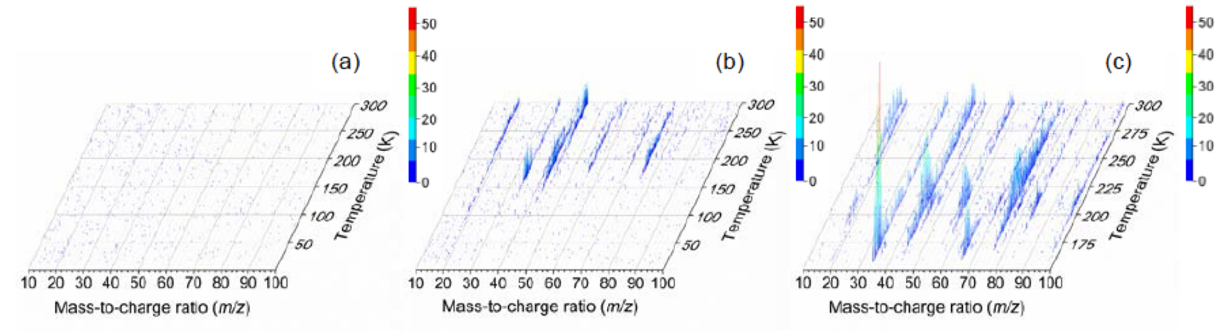

Figure 1. Mass-to-charge dependent TPD profiled obtained after photoionization (10.49 eV) molecule desorbed from the Murchison samples: a) blank, b) dual irradiation at 5 K, and c) dual irradiation at 150 K.

and H_2S_2 than the low temperature experiments by factors of 4.1 ± 0.5 and 10.5 ± 1.0, respectively. In addition, these dual irradiation experiments did yield evidence for the formation of water via the ν_3 asymmetric stretching at 3.0 µm (3332 cm^{-1}) and 3.3 µm (3151 cm^{-1}) [19]. There also was a small peak for CO_2 around (2350 cm^{-1}). PI-ReTOF-MS data taken during TPD also support formation of these species (*m/z*= 20 and 44).

The signals from *m/z* = 34 and 36 in Figure 1 can be assigned to hydrogen sulfide: $H_2{}^{32}S$ and $H_2{}^{34}S$, respectively [20]. These assignments are confirmed in part by the ratio of the integrated areas of signal at *m/z*=36 and 34, which is 0.049 ± 0.005 and closely matches the natural abundance ratio of ^{34}S and ^{32}S (0.045) [21]. The ion signals at *m/z* = 64, 66, and 68 can be assigned to hydrogen disulfide: $^{32}S_2$, $H_2{}^{32}S_2$, and $H_2{}^{32}S^{34}S$, respectively [20]. The ratio of integrated area of *m/z* = 68 and 66 is 0.092 ± 0.009, which is consistent with the natural abundance ratio of $H_2{}^{32}S_2$ and $H_2{}^{32}S^{34}S$ (0.089).

Energetic electrons easily break weak chemical bonds like Fe−S and S−H; thus generating suprathermal sulfur and hydrogen atoms [22]. Since these atoms have excess kinetic energies, diffuse recombination reactions such as $H + S \rightarrow HS$, $HS + H \rightarrow H_2S$, and $HS + HS \rightarrow H_2S_2$ can proceed even at temperatures as low as 5 K [20]. Hydrogen sulfide may also serve as a precursor to H_2S_2. Once formed within the sample, the simulated micrometeorite impact likely induces thermal diffusion of the sulfur-bearing molecules to the surface, where they may sublime during the TPD phase. The greater abundance of H_2S and H_2S_2 generated for the higher temperature irradiation is likely caused by enhanced thermal diffusion, which leads to more surface H_2S and H_2S_2 [20]. Further, the laser can also vibrationally excite the C−H and Fe−S stretches in the electron exposed sample. It has been reported that the bond rupture processes and reactions of vibrationally excited molecules are considerably enhanced compare to their counterpart in the vibrational ground state [23]. This effect may enrich the energetic sulfur and hydrogen atoms in the sample and therefore produce more H_2S and H_2S_2 [20].

Based on these results we suggest that sulfur on the surface of C-complex asteroids (<500 km) and by inference S-complex asteroids, may be depleted in sulfur via generation of volatile H_2S and H_2S_2 by surfaces encountering energetic electrons and micrometeorite impacts.

Conclusions: This laboratory study details the formation of H_2S and H_2S_2 from conversion of non-volatile sulfuretted species in the Murchison meteorite. The results indicate that space weathering processes likely induce depletion of sulfur on the surface of C-type and undifferentiated S-type asteroids. We predict that the forthcoming C-complex asteroid sample-return missions: OSIRIS-Rex and Hayabusa 2 will detect sulfur depletion on the surfaces of asteroids Bennu and Ryugu, respectively. Furthermore, as H_2S and H_2S_2 will sublime when the samples from asteroids are allowed to reach temperatures higher than 150 K and H_2S_2 is unstable at ambient temperatures on Earth, cryogenic curation of the samples is necessary to keep scientific integrity of these fragile species [24].

References: [1] Pieters, C.M. et al., 2000, *MAPS*, **35**, 1101-1107; [2] Hapke, B. 2001, *JGR,* **106**, 10039; [3] Chapman, C. 2004, *Annu. Rev. Earth Planet. Sci.,* **32**, 539; [4] Gaffey, M. J., 2010. *Icarus*. **209**, 564-574; [5] Pieters, C. M., Noble, S. K., 2016. *JGR: Planets*. **121,** 1865-1884; [6] Clark, B. E., et al. 2002. *Asteroids III*. University of Arizona Press, Tucson, pp. 585–599; [7] Haskin, L. A., Warren, P. H. 1991., *Lunar Source Book*, Cambridge University Press, Cambridge [England]; New York, pp. 357-474. [8] Gillis-Davis, J.J. and Scott, E. R. D. 2014. *LPSC 45*, Abstract #1189; [9] Loeffler, M., et al. 2008. *Icarus*. **195,** 622-629; [10] Killen, R., 2003. *MAPS*. **38**, 383-388; [11] Nittler, L. R., et al., 2004. Antarct. Meteorite Res. **17,** 231-251; [12] Jarosewich, E., 1990, *MAPS*, **25**, 323; [13] Trombka, J. I. et al., 2000, *Science*, **289**, 2101; [14] Nittler, L. R., et al., 2001. *MAPS*, **36**, 1673-1695; [15] McCoy, T. J., et al., 2002. *Chem. Erde*, **62**, 89-121; [16] Nittler, L. R., 2014. *Elements*. **10**, 51-52; [17] Arai, T., et al. 2008. *EP&S*, **60,** 21-31; [18] Keller, L. P., Berger, E. L., 2014. *EP&S*. **66**, 71-78; [19] Gillis-Davis et al. 2018, *LPSC 49*, Abstract #2051; [20] C. Zhu et al. 2019, *submitted to JGR-Planets*; [21] Cooper, G. W., et al. 1992. *GCA*. **56,** 4109-4115; [22] Bennett, C. J., et al. 2006. *Astrophysical Journal*. **653,** 792. [23] Palma, J., et al. 2002. *CPL*. **363,** 529-533; [24] Mitchell, J., et al. 2018. *LPSC 49*, Abstract #1019.